Available online at www.sciencedirect.com
ScienceDirect
Tetrahedron
Tetrahedron 63 (2007) 11093–11100

Zn^{2+} selective luminescent '*off–on*' probes derived from diaryl oxadiazole and aza-15-crown-5

Sabir H. Mashraqui,[a,*] Subramanian Sundaram,[a] Tabrez Khan[a] and A. C. Bhasikuttan[b]

[a]*Department of Chemistry, University of Mumbai, Vidyanagari, Santacruz-E, Mumbai 400098, Maharashtra, India*
[b]*Radiation and Photochemistry Division, Bhabha Atomic Research Centre, Mumbai 400085, Maharashtra, India*

Received 28 April 2007; revised 25 July 2007; accepted 10 August 2007
Available online 15 August 2007

Abstract—New photo-induced electron transfer (PET) probes **OMOX** and **OBOX**, carrying an additional binding site in the form of 'oxadiazole nitrogen' have been designed to evaluate binding interactions with biologically significant Li^+, Na^+, K^+, Ca^{2+}, Mg^{2+}, and Zn^{2+} including environmentally toxic Ba^{2+} and Cd^{2+} using optical spectral techniques. While Li^+, Na^+, and K^+ did not appreciably perturb either the absorption or emission spectra, Ba^{2+}, Ca^{2+}, Mg^{2+}, Zn^{2+}, and Cd^{2+} induced slight red shifts (2–8 nm) in the UV–visible spectra as well as pronounced chelation induced enhanced fluorescence (CHEF). Both **OMOX** and **OBOX** exhibited the highest CHEF in contact with the zinc ion, whereas Ba^{2+}, Ca^{2+}, Mg^{2+}, and Cd^{2+} induced relatively less emission enhancements. **OBOX**, which is a poorer emitter (Φ_f=0.0062) than **OMOX** (Φ_f=0.015), showed highly promising 160-fold emission enhancement in the presence of Zn^{2+}. Potential, therefore is available in **OBOX** to function as a selective luminescent '*off–on*' sensor for Zn^{2+} in the presence of coordinatively competing Ba^{2+}, Ca^{2+}, Mg^{2+}, and Cd^{2+} ions.

1. Introduction

Designing functional luminescent probes for the selective detection of chemically and biologically significant metal ions continues to engage worldwide attention. Given the diverse roles of Zn^{2+} in a multitude of cellular functions, its trace detection is of special interest. Zinc ion is implicated as a structural cofactor in metalloproteins, regulation of gene expression,[1] and cellular apoptosis.[2] Zn^{2+} is also a constituent of most DNA and RNA polymerases.[3] A disorder of zinc metabolism is believed to give rise to many neurological conditions such as Alzheimer's disease, amyotrophic lateral sclerosis, Guam ALS-Parkinsonism dementia, and hypoxia-ischemia and epilepsy.[4] Additionally, clinical evidence shows that zinc nutrition aids in wound healing through a family of zinc dependent endopeptidases.[5] Also, zinc metal is a soil pollutant, significant concentrations of which cause phytotoxic effects on soil microbes.[6]

Most zinc sensors typically operate via PET, a process that induces CHEF upon metal ion coordination with the aza-receptor domains. Some well-known Zn^{2+} probes include aryl sulfonamide derivatives of 8-aminoquinoline, such as 6-methoxy-(8-*p*-toluenesulfonamido)quinoline,[7] Zinquin,[8] Zinbo-5,[9] and the Zinpyr family of chemosensors.[10] Luminescent zinc sensors have also been designed using high zinc affinity ligands, e.g., dipicolyl amine,[10c,11] cyclam,[11f,h] and iminodiacetic acid.[12] However, with a few exceptions,[12a,13] most Zn^{2+} probes provide fewer than 15-fold CHEF upon zinc coordination.[11d,14] Moreover, optical spectral interference arising from the coordinatively competing Ba^{2+}, Ca^{2+}, Mg^{2+}, and Cd^{2+} ions are a mitigating factor, which limit the application of these sensors.[11f,h,15] Therefore, selective discrimination of zinc ions is still deemed an appealing area of research.[12e,f,14b,c,e,16]

Though, monoaza-15-crown-5 is known to bind zinc ion, surprisingly Zn^{2+} sensors incorporating this receptor are scarce in the literature.[13a,16a,17] In the context of our interest in fluoroionophores,[18] we recently reported a new class of PET based sensors, **MOX** and **BOX** (Scheme 1). These probes were selective for Mg^{2+} among selected alkali and divalent metal ions examined by us.[19] However, in **MOX** and **BOX**, only the aza-crown ring(s) participate in metal ion complexation, with conceivably no binding interaction stemming from the remotely placed oxadiazole. Since, participation of the nitrogen of the oxadiazole ring in metal ion coordination is precedented,[20] we have presently designed new analogs, designated as **OMOX** and **OBOX** with a view to inducing lariat-type participation of oxadiazole in the complexation process. Structurally, fluoroionophores

Keywords: Diaryl oxadiazoles; Synthesis; Photo-induced electron transfer; UV–visible; Fluorescence; Selective Zn^{2+} sensor.
* Corresponding author. Tel.: +91 022 26526091; fax: +91 022 26528547; e-mail: sh_mashraqui@yahoo.com

0040–4020/$ - see front matter © 2007 Elsevier Ltd. All rights reserved.
doi:10.1016/j.tet.2007.08.031

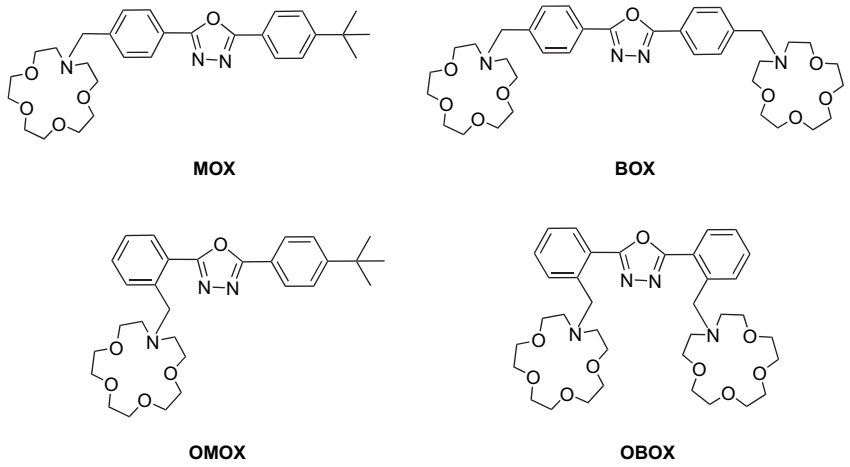

Scheme 1.

OMOX and **OBOX** are characterized by the presence of one and two aza-15-crown-5 receptors at the 2 and 2,2′ positions of the diaryl-oxadiazole motif, respectively. The photophysical behaviors of **OMOX** and **OBOX**, being fluorophore-spacer-receptor models, are expected to be governed by the PET mechanism. Furthermore, the availability of additional ligating site in the form of 'oxadiazole nitrogen' in **OMOX** and **OBOX**, (a feature lacking in **MOX** and **BOX**) is expected to alter their metal binding characteristics to offer different or improved photo-physical responses in the company of interacting metal ions.

2. Results and discussion

Synthesis of **OMOX** and **OBOX** was carried out as shown in Scheme 2. Condensation of *o*-toluolyl chloride **1** with 4-*tert*-butylbenzoic hydrazide **2** in refluxing $POCl_3$ provided diaryl oxadiazole **3** in good yield. Bromination of **3** with NBS/CCl_4 containing a catalytic amount of dibenzoyl peroxide afforded bromide **4**. The reaction of **4** with a slightly more than 1 equiv of monoaza-15-crown-5 under acetonitrile/K_2CO_3 condition, followed by SiO_2 column purification afforded **OMOX** as a light yellow oil. Toward the synthesis of **OBOX**, *o*-toluolyl chloride **1** was condensed with *o*-toluic hydrazide **5** in $POCl_3$ under reflux. The resulting oxadiazole **6** was subjected to two-fold bromination with NBS/CCl_4 containing a catalytic amount of dibenzoyl peroxide to afford dibromide **7**. Finally, the coupling of **7** with 2.2 equiv of monoaza-15-crown-5 under the conditions described for **OMOX** gave after SiO_2 purification **OBOX** as light yellow oil.

Absorbance spectra of **OMOX** (Fig. 1) and **OBOX** (Fig. 2) measured in MeCN showed a broad band at 275 and 270 nm, with molar extinction coefficients, ε_m of ca. 2.31×10^4 and $2.52\times10^4\ M^{-1}\ cm^{-1}$, respectively. Addition of perchlorates of Li^+, Na^+, K^+, Ba^{2+}, Ca^{2+}, Mg^{2+}, Zn^{2+}, and Cd^{2+} to the solutions of **OMOX** and **OBOX** in MeCN produced small red shifts of 1–8 nm. Since, the PET sensors do not exhibit ground state interactions between the receptor and the fluorophore, their excitation energies remain essentially unperturbed upon exposure to metal ions. However, in the cases of **OMOX** and **OBOX**, which are also PET probes, the observed small red shifts, particularly with Zn^{2+} (8 nm), Mg^{2+} (6 nm), and Cd^{2+} (5 nm) could be a consequence of lariat-type binding of the oxadiazole nitrogen with the aza-crown-bound cations. Such an interaction could induce a marginal degree of enhancement in the charge transfer interaction between the donor aryl ring(s) and the acceptor, metal-coordinated oxadiazole, thereby giving rise to the slight red shifts.

Excitation of **OMOX** and **OBOX** at their absorption maxima at 275 and 270 nm produced, respectively, emission bands at 356 and 339–350 nm regions. These emission bands presumably originate from the locally excited states. The quantum yields Φ_f for **OMOX** and **OBOX**, determined with reference to 2,2′-biphenyldiol in acetonitrile (Φ_f=0.29)[21] were found to be 0.0150 and 0.0062, respectively. Relatively poor Φ_f for **OBOX** compared to **OMOX** is understandable in view of a more efficient PET quenching arising from two aza-crown ether rings in **OBOX** as against just one aza-crown ether quencher in **OMOX**. This behavior is in accord with many known fluoroionophores carrying bis-(aza)-crown ether, which also display highly quenched fluorescence.[19,22]

Consistent with the red shifts observed in the UV spectra, the emission bands of **OMOX** and **OBOX** (λ_{em} at 356 and 350 nm, respectively) were also slightly red shifted by 1–5 nm upon adding perchlorates of Li^+, Na^+, K^+, Ba^{2+}, Ca^{2+}, Mg^{2+}, Zn^{2+}, and Cd^{2+}. Fluorescence emission changes of **OBOX** with respect to increasing concentration of Zn^{2+} are depicted in Figure 3. With alkali metal ions Li^+, Na^+, K^+ (concn $\geq$100-fold, i.e., $\geq2.97\times10^{-4}$ M) emission-band intensities increased only ca. 3–50%, however Ba^{2+}, Ca^{2+}, Mg^{2+}, Zn^{2+}, and Cd^{2+} induced significantly higher chelation induced enhanced fluorescence (CHEF) at relatively lower concentrations ($\leq1.18\times10^{-5}$ M) in the emission spectra of both **OMOX** and **OBOX**. In the presence of Ba^{2+}, Ca^{2+}, Mg^{2+}, Zn^{2+}, and Cd^{2+}, the CHEF experienced by **OMOX** and **OBOX** were found to be 4.6, 8.5, 14.6, 30.0, and 11.0-folds and 7.5, 3.4, 28.0, 160.0, and 43.0-fold, respectively. The fluorescence enhancements observed with **OMOX** in the presence of various metal ions follow the order

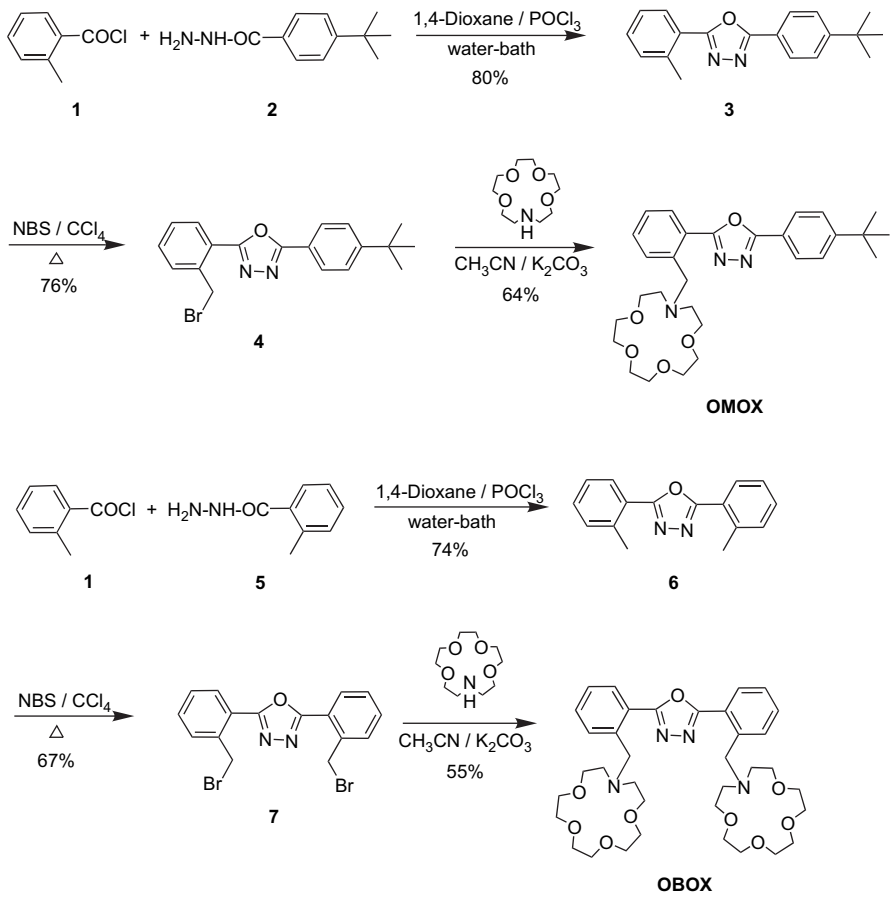

Scheme 2.

$Zn^{2+}>Mg^{2+}>Cd^{2+}>Ca^{2+}>Ba^{2+}>Li^{+}\cong Na^{+}\cong K^{+}$ while for **OBOX**, the order is $Zn^{2+}\gg Cd^{2+}>Mg^{2+}>Ba^{2+}>Ca^{2+}>Li^{+}>K^{+}>Na^{+}$. With the aza-crown receptor being common to both hosts, the marked differences observed in the binding profiles with different metal ions presumably reflect differing degree of participation of the oxadiazole nitrogen with the aza-crown bound metal ions. The relative fluorescent enhancements observed with **OMOX** and **OBOX** with various metal ions at their complete complexations are highlighted in Figures 4 and 5, respectively. Of particular note is the observation that among various cations examined, zinc ion in both **OMOX** and **OBOX** produced the highest CHEF by a factor of 30 and 160-fold, respectively. Furthermore, **OBOX**, which is a poorer emitter than **OMOX** (Φ_f

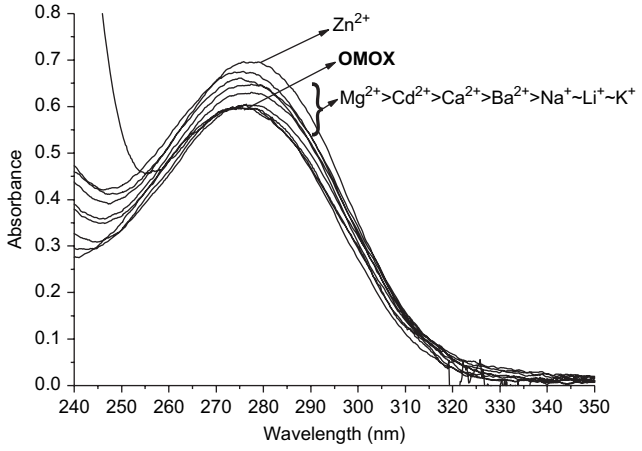

Figure 1. Absorption spectra of **OMOX** (2.55×10^{-5} M) in the absence and presence of Li^{+} (5.35×10^{-5} M), Na^{+} (4.84×10^{-5} M), K^{+} (5.86×10^{-5} M), Ba^{2+} (4.33×10^{-5} M), Ca^{2+} (3.98×10^{-5} M), Mg^{2+} (3.95×10^{-5} M), Zn^{2+} (2.80×10^{-5} M), and Cd^{2+} (2.89×10^{-5} M) perchlorates at their saturated concentration in MeCN.

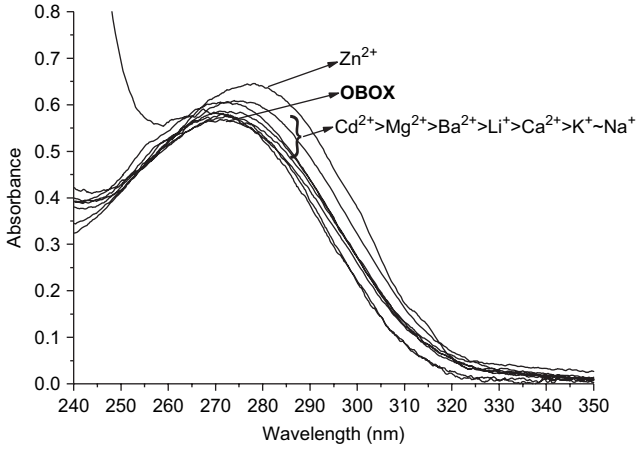

Figure 2. Absorption spectra of **OBOX** (2.17×10^{-5} M) in the absence and presence of Li^{+} (7.48×10^{-5} M), Na^{+} (7.38×10^{-5} M), K^{+} (7.59×10^{-5} M), Ba^{2+} (6.48×10^{-5} M), Ca^{2+} (6.42×10^{-5} M), Mg^{2+} (6.18×10^{-5} M), Zn^{2+} (5.86×10^{-5} M), and Cd^{2+} (6.08×10^{-5} M) perchlorates at their saturated concentration in MeCN.

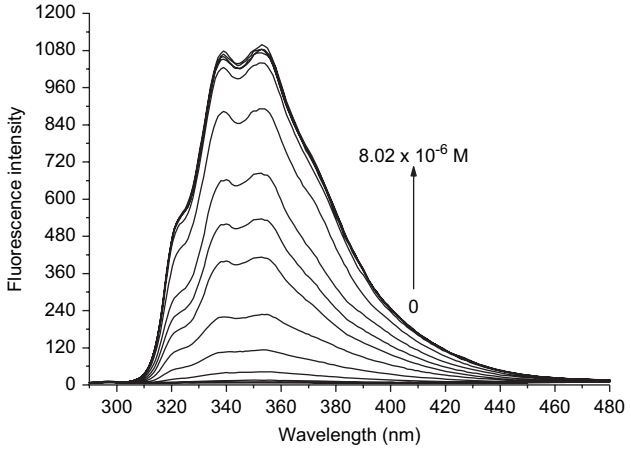

Figure 3. Fluorescence spectra (corrected) of **OBOX** (2.97×10^{-6} M) on titration with Zn^{2+} (0–8.02×10^{-6} M) in MeCN.

of 0.0062 vs 0.0150) showed, except for Ca^{2+} relatively higher emission enhancements with the other divalent metal ions examined. This behavior is due to a more efficient suppression of PET process in **OBOX** as a consequence of blocking of electron transfer from both the aza-crown ether domains. Similar results have been previously encountered with certain diaza-crown ethers, which also exhibit significantly higher fluorescence switch-on ability on complexation compared to their monoaza-crown counterparts.[23] The selectivity ratios for zinc ions, expressed as Zn^{2+}/M^{2+} for **OMOX** with respect to interfering Ba^{2+}, Ca^{2+}, Mg^{2+}, and Cd^{2+} were found to be 6.5, 3.5, 2.1, and 2.7, respectively. However, the corresponding selectivity ratios for **OBOX** are significantly higher at 21.5, 46.6, 5.7, and 3.7, respectively. Clearly, **OBOX**, compared to **OMOX** exhibits better selectivity and improved optical discrimination for the zinc ion relative to coordinatively interfering Ba^{2+}, Ca^{2+}, Mg^{2+}, and Cd^{2+} ions.

Addition of ca.1 equiv of Zn^{2+} to a solution of **OMOX** in CH_3CN led to an approximate plateau indicating 1:1 complexation stoichiometry (Fig. 6), which was further confirmed by applying the Job's plot method. On the other

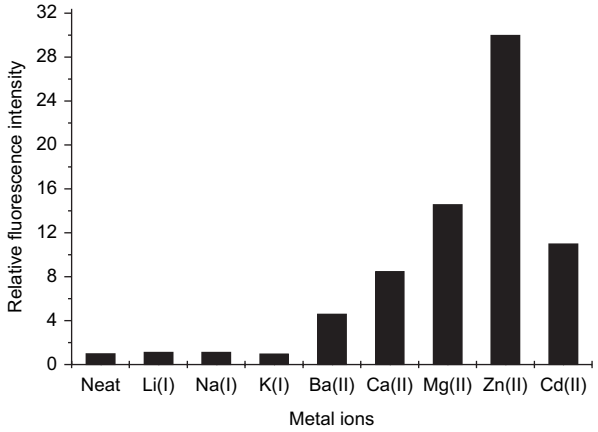

Figure 4. The relative fluorescence intensity of **OMOX** (6.96×10^{-6} M) on addition of Li^{+} (1.46×10^{-5} M), Na^{+} (1.32×10^{-5} M), K^{+} (1.59×10^{-5} M), Ba^{2+} (1.18×10^{-5} M), Ca^{2+} (1.08×10^{-5} M), Mg^{2+} (1.08×10^{-5} M), Zn^{2+} (7.64×10^{-6} M), and Cd^{2+} (7.89×10^{-6} M) perchlorates at their saturated concentration (λ_{ex}=275 nm, λ_{em}=356 nm) in MeCN.

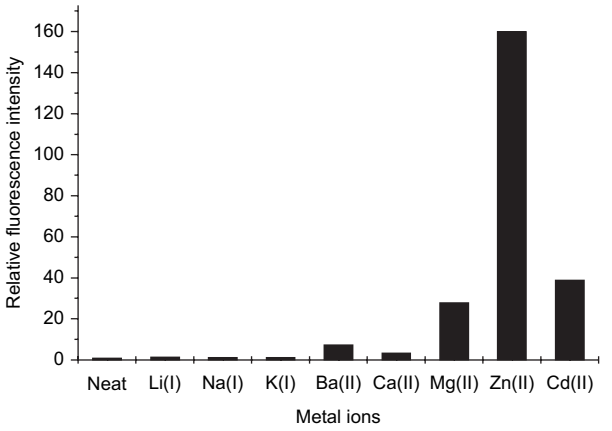

Figure 5. The relative fluorescence intensity of **OBOX** (2.97×10^{-6} M) on addition of Li^{+} (1.02×10^{-5} M), Na^{+} (1.01×10^{-5} M), K^{+} (1.04×10^{-5} M), Ba^{2+} (8.88×10^{-6} M), Ca^{2+} (8.79×10^{-6} M), Mg^{2+} (8.46×10^{-6} M), Zn^{2+} (8.02×10^{-6} M), and Cd^{2+} (8.32×10^{-6} M) perchlorates at their saturated concentration, (λ_{ex}=270 nm, λ_{em}=350 nm).

hand, for **OBOX**, which contains two aza-crown receptors, an approximate plateau is reached at ca. 2.7 equiv of Zn^{2+} ions (see the plot shown in Fig. 7). Unlike **OMOX**, where 1 equiv of Zn^{2+} produced the highest (30-fold) emission enhancement, however, in contrast for the case of **OBOX**, addition of ca. 1 equiv of zinc resulted in only a six-fold enhancement in emission intensity. This observation implies that when only one aza-crown is metal bound, the PET process still remains substantially operative due to the non-occupancy of the second aza-crown ring. It is only when the Zn^{2+} concentration is increased beyond 1 equiv that steeper increases in emission intensity are observed, reaching a maximum of 160-fold at ca. 2.7 mole fraction of zinc. In this case, 1:2 stoichiometry corresponding to **OBOX** and Zn^{2+} was indicated by the Job's plot method. Ideally, we expected to observe two plateaus for **OBOX**, the first plateau appearing at 1:1 and the second at 1:2 stoichiometry with respect to **OBOX** and Zn^{2+}. However, in practice only a single plateau corresponding to approximately 1:2 stoichiometry was discernible in this case. Failure to observe two separate plateau could in parts be due to (a) the formation of small amount of 1:2 complex even at 1:1 stoichiometry and (b) relatively steeper increases in

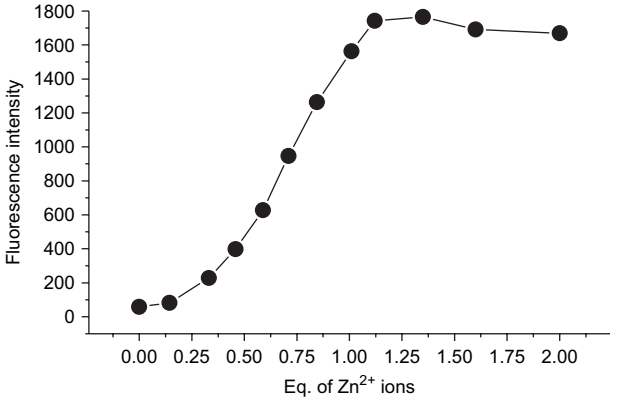

Figure 6. Variation in fluorescence intensity of a solution of **OMOX** (6.96×10^{-6} M) in MeCN at 356 nm as a function of added equivalents of Zn^{2+}.

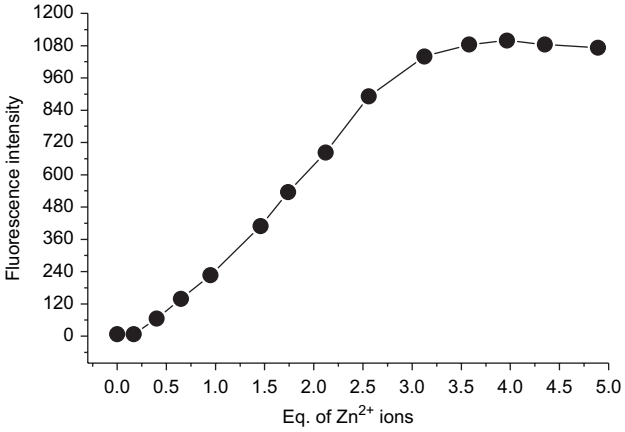

Figure 7. Variation in fluorescence intensity of a solution of **OBOX** (2.97×10^{-6} M) in MeCN at 350 nm as a function of added equivalents of Zn^{2+}.

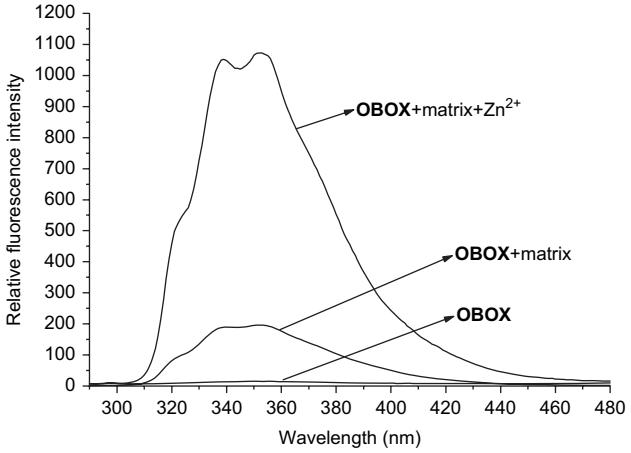

Figure 8. Fluorescence spectra of **OBOX** alone (2.97×10^{-6} M), **OBOX**+matrix, consisting of Ba^{2+} (8.88×10^{-6} M), Ca^{2+} (8.79×10^{-6} M), Mg^{2+} (8.46×10^{-6} M), and Cd^{2+} (8.32×10^{-6} M), at their complete complexation and **OBOX**+above matrix+$Zn(ClO_4)_2$ (8.02×10^{-6} M) in MeCN.

the emission intensity beyond 1:1 complexation stoichiometry. These factors together could obscure the first plateau expected at 1:1 complexation stoichiometry.

Apparent stability constants (log K_s), derived from emission intensity changes for **OMOX** and **OBOX** with different cations are compiled in Table 1. For alkali metal ions, fluorescence changes were too small to allow a reliable measure of their log K_s. Relatively poor CHEF with alkali metal ions could be ascribed to their weak affinities toward the aza-crown ring. Significantly higher log K_s of 6.95 for Zn^{2+} compared to Ca^{2+} and Mg^{2+} (log $K_s\leq5.89$) obtained with the better of the two fluoroionophore, **OBOX** is an important factor in favor of zinc discrimination since, under many physiological conditions, Ca^{2+} and Mg^{2+} exist at relatively higher concentration than Zn^{2+}. Remarkably high recognition of Zn^{2+} compared to the divalent ions investigated could presumably arise from relatively stronger binding of Zn^{2+} with the aza-crown ether to effectively block the PET process. In addition, electrostatic interaction of the aza-crown bound Zn^{2+} with the 'oxadiazole nitrogen' could cause restricted rotation around the aryl-oxadiazole bonds, thereby reinforcing the radiative return of the excited states over that of the non-radiative deactivation.

To substantiate the high preference for Zn^{2+} in the presence of interfering cations, fluorescence spectra of **OBOX** (2.97×10^{-6} M) were recorded both without and with a matrix consisting of Ba^{2+}, Ca^{2+}, Mg^{2+}, and Cd^{2+} at their complete complexation. The fluorescent spectrum with the matrix revealed ca. 40-fold emission enhancement in the fluorescence spectrum of **OBOX** (Fig. 8). This emission enhancement is reminiscent of that observed with Cd^{2+}, which is one of the strongest complexing cations present in the matrix. Upon adding $Zn(ClO_4)_2$ (8.02×10^{-6} M) to the above matrix, we observed a jump in the fluorescence enhancement by ca. 120-fold, the overall enhancement being 160-fold, the same as measured with Zn^{2+} alone (see Fig. 3). Evidently, the superior complexing zinc ion displaces the relatively poorly interacting Ca^{2+}, Ba^{2+}, Mg^{2+}, and Cd^{2+} to form the corresponding **OBOX**–Zn^{2+} complex.

3. Conclusions

New PET based fluoroionophores, **OMOX** and **OBOX** have been synthesized and their absorption and emission characteristics investigated in the presence of biologically important alkali and alkaline earth metal ions, including toxic

Table 1. Relative quantum yield (Φ_f), CHEF, and log K_s of **OMOX** and **OBOX** in the presence of metal ions

M^{n+}	OMOX			OBOX		
	Φ_f[a]	CHEF	log K_s[b]	Φ_f[a]	CHEF	log K_s[b]
Free	0.0150	1	—	0.0062	1	—
Li^+	0.0169	1.13	*[c]	0.0233	1.52	*[c]
Na^+	0.0166	1.11	*[c]	0.0105	1.22	*[c]
K^+	0.0145	1.03	*[c]	0.0124	1.37	*[c]
Ba^{2+}	0.0675	4.60	5.12±0.12	0.0434	7.45	4.92±0.12
Ca^{2+}	0.1200	8.50	5.35±0.18	0.0201	3.43	4.60±0.19
Mg^{2+}	0.2085	14.58	5.73±0.21	0.1670	28	5.27±0.17
Zn^{2+}	0.4200	30	6.05±0.17	0.9553	160	6.95±0.14
Cd^{2+}	0.1575	11	5.60±0.14	0.2616	43	5.89±0.12

[a] The fluorescence quantum yields (Φ_f) were determined by comparing the integrated fluorescence spectra of the samples with that of the reference 2,2′-biphenyldiol in acetonitrile (Φ_f=0.29).[21]
[b] The stability constants were determined by non-linear fitting curve of fluorescence data.[24]
[c] log K_s could not be determined due to insignificant fluorescence enhancement.

and polluting Ba^{2+} and Cd^{2+}. While, the absorption spectra are only marginally modified when exposed to various metal ions, significant emission enhancements were however detected only in the presence of divalent cations. In particular, the highest emission enhancements were observed for both **OMOX** and **OBOX** upon contact with Zn^{2+}. The CHEF of 160-fold experienced by **OBOX** with Zn^{2+} is the one of the highest among the known PET based Zn^{2+} sensors. Although not yet defined, the participatory role of 'oxadiazole nitrogen' in the complexation process could be a factor in contributing to high fluorescence enhancements by imposing conformational rigidity on the host molecules. The dramatic increase in the emission-band intensity and high optical discrimination render **OBOX**, the better of the two hosts a potential interesting luminescent '*off–on*' probe for Zn^{2+} in the presence of interfering Ca^{2+}, Mg^{2+}, Ba^{2+}, and Cd^{2+} ions.

4. Experimental

4.1. General

Metal perchlorates were prepared as described in the literature[25] and dried under vacuum prior to use. The chemicals and spectral grade solvents were purchased from S. D. fine Chemicals (India) and used as received. IR spectra were recorded on a Shimadzu FTIR-420 spectrophotometer. ^{1}H NMR spectra were recorded in $CDCl_3$ solution on a 300 MHz Bruker-AMX-500 spectrometer with TMS as an internal standard. Coupling constants *J* are given in hertz. ^{13}C NMR spectra (75.5 MHz) were recorded on a Bruker AC-300 instrument. Mass spectra were obtained using LC–MS in ESI mode. Elemental analyses were done on Carlo Erba instrument EA-1108 Elemental analyzer. UV–visible spectra were recorded on a Jasco V-530 UV–visible spectrophotometer and fluorescence spectra were recorded on Hitachi F-4500 Fluorescence spectrophotometer. The fluorescence quantum yields (Φ_f) were determined by comparing the integrated fluorescence spectra of the sample with 2,2′-biphenyldiol in MeCN (Φ_f=0.29).[21]

4.1.1. 2-(2-Methylphenyl)-5-(4-*tert*-butylphenyl)-1,3,4-oxadiazole (3). *o*-Toulic acid (3.40 g, 25 mmol) was taken in benzene, to it was added $SOCl_2$ (2.14 mL, 30 mmol) and refluxed for about 2 h. Benzene and excess $SOCl_2$ were removed by vacuum distillation. The resultant acid chloride **1** was dissolved in dry 1,4-dioxane and 4-*tert*-butylbenzoic hydrazide **2** (4.61 g, 24 mmol) was introduced. The reaction mixture was heated on water-bath for about 2 h, till evolution of HCl gas ceased. To the reaction mixture was then added $POCl_3$ and the reaction continued to be heated on water-bath for 3 h, till evolution of HCl gas ceased. The reaction was brought to room temperature and poured carefully into 100 mL of ice-cold water and neutralized with Na_2CO_3 to get a precipitate. The solid was filtered, washed with water, and air-dried. Crystallization from methyl alcohol gave **3** as a colorless crystalline solid in 80% yield (5.60 g), mp 80–83 °C. IR (KBr, ν, cm^{-1}): 3074, 2960, 1614, 1582, 1540, 1497, 1268, 1115, 1052, 847, 777, 727, 669, 560. ^{1}H NMR (300 MHz, $CDCl_3$): δ 8.07 (d, *J*=8.4 Hz, 2H, Ar–*H*), 8.03 (d, *J*=6.6 Hz, 1H, Ar–*H*), 7.56 (d, *J*=8.4 Hz, 2H, Ar–*H*), 7.46–7.34 (m, 3H, Ar–*H*), 2.77 (s, 3H, Ar–CH_3), 1.38 (s, 9H, Ar–C(CH_3)$_3$). *m*/*z*: 293 (M+1)$^+$, 275, 252, 211, 161, 137. Anal. Calcd for $C_{19}H_{20}N_2O$: C, 78.08; H, 6.85; N, 9.59. Found: C, 77.98; H, 7.05; N, 9.74%.

4.1.2. 2-[2-(Bromomethyl)phenyl]-5-(4-*tert*-butylphenyl)-1,3,4-oxadiazole (4). Oxadiazole **3** (3 g, 10.28 mmol) and *N*-bromosuccinimide (NBS) (2.19 g, 1.2 equiv) were dissolved in carbon tetrachloride. A catalytic amount of benzoyl peroxide (BPO) was added as an initiator and the reaction mixture refluxed for about 5 h. The reaction mixture was brought to room temperature and the insoluble succinimide filtered off. The filtrate was concentrated to give crude solid. Crystallization from methanol gave **4** as a colorless solid in 76% yield (2.89 g), mp 117–119 °C. IR (KBr, ν, cm^{-1}): 3055, 2957, 1613, 1541, 1494, 1440, 1267, 1221, 1105, 1016, 845, 756, 712, 601, 557. ^{1}H NMR (300 MHz, $CDCl_3$): δ 8.11 (d, *J*=8.1 Hz, 2H, Ar–*H*), 7.61–7.49 (m, 6H, Ar–*H*), 5.16 (s, 2H, Ar–CH_2Br), 1.38 (s, 9H, Ar–C(CH_3)$_3$). *m*/*z*: 372 (M+1)$^+$, 342, 329, 315, 289, 274, 258, 211, 181, 137. Anal. Calcd for $C_{19}H_{19}BrN_2O$: C, 61.45; H, 5.12; N, 7.55; Br, 21.56. Found: C, 61.75; H, 5.37; N, 7.43; Br, 21.47%.

4.1.3. *N*-[2-(4-Methylphenyl)-5-(4-*tert*-butylphenyl)-1,3,4-oxadiazole]aza-15-crown-5 (OMOX). Bromide **4** (0.371 g, 1 mmol) and monoaza-15-crown-5 (0.263 g, 1.2 mmol) were dissolved in dry acetonitrile. After the addition of anhyd K_2CO_3 (250 mg), the reaction mixture was stirred and refluxed on water-bath for about 3 h. The reaction mixture was then filtered and the filtrate concentrated. The brown oily mass obtained was extracted with chloroform, washed with water, and dried over Na_2SO_4. Crude product obtained on solvent removal was purified by SiO_2 column chromatography (R_f=0.27) using $CHCl_3$:CH_3OH (99:1) as an eluent. The compound **OMOX** was obtained as pale yellow oil in 64% yield (0.326 g). IR (Nujol, ν, cm^{-1}): 2962, 2870, 1614, 1547, 1496, 1415, 1362, 1250, 1128, 935, 844, 751, 716. ^{1}H NMR (300 MHz, $CDCl_3$): δ 8.06 (d, *J*=8.5 Hz, 2H, Ar–*H*), 7.91 (d, *J*=7.5 Hz, 1H, Ar–*H*), 7.78 (d, *J*=7.6 Hz, 1H, Ar–*H*), 7.55 (d, *J*=8.5 Hz, 2H, Ar–*H*), 7.51 (t, *J*=7.5 Hz, 1H, Ar–*H*), 7.39 (t, *J*=7.6 Hz, 1H, Ar–*H*), 4.15 (s, 2H, >NCH_2–Ar), 3.63–3.51 (m, 16H, –OCH_2CH_2–), 2.77 (t, 4H, *J*=8.2 Hz, >NCH_2CH$_2$O–), 1.37 (s, 9H). ^{13}C NMR ($CDCl_3$): δ 164.90, 164.36, 155.27, 131.22, 130.29, 129.60, 127.10, 126.73, 126.07, 123.14, 121.19, 70.96, 70.84, 70.48, 70.11, 69.88, 59.10, 54.69, 35.08, 31.12. *m*/*z*: 511 (M+2)$^+$, 467, 423, 373, 335, 292, 241, 219, 162. Anal. Calcd for $C_{29}H_{39}N_3O_5$: C, 68.37; H, 7.66; N, 8.25. Found: C, 68.07; H, 7.89; N, 8.44%.

4.1.4. 2,5-Bis(2-methylphenyl)-1,3,4-oxadiazole (6). *o*-Toulic acid (3.40 g, 25 mmol) was converted into acid chloride **1** as described earlier. The crude acid chloride **1** and *o*-toluic hydrazide **5** (3.60 g, 24 mmol) were dissolved in dry 1,4-dioxane (50 mL) and the reaction mixture heated on a water-bath for about 2 h, till evolution of HCl gas ceased. $POCl_3$ (10 mL) was then introduced and the reaction continued to be heated on the water-bath for further 3 h. The reaction was poured carefully into 100 mL of ice-cold water, neutralized with Na_2CO_3, filtered, and dried. Crystallization of the crude with methyl alcohol gave **6** as a colorless solid in 74% yield (4.44 g), mp 120–122 °C. IR (KBr, ν, cm^{-1}):

3040, 2959, 1604, 1535, 1449, 1386, 1247, 1051, 1035, 782, 729, 678, 561. ^{1}H NMR (300 MHz, $CDCl_3$): δ 8.05 (d, J=7.8 Hz, 2H, Ar–*H*), 7.47–7.34 (m, 6H, Ar–*H*), 2.79 (s, 6H, Ar–C(CH_3)$_3$). *m/z*: 251 (M+1)$^+$, 238, 223, 209. Anal. Calcd for $C_{16}H_{14}N_2O$: C, 76.80; H, 5.60; N, 11.20. Found: C, 77.05; H, 5.74; N, 10.96%.

4.1.5. 2,5-Bis[2-(bromomethyl)phenyl]-1,3,4-oxadiazole (7). A mixture of **6** (3.75 g, 15 mmol) and *N*-bromosuccinimide (NBS) (5.73 g, 2.2 equiv) was dissolved in carbon tetrachloride. A catalytic amount of BPO was added as an initiator. The reaction mixture was refluxed for about 5 h whereby the reaction was judged to be complete by TLC. The reaction mixture was filtered to remove succinimide. The filtrate was concentrated to give a crude solid. Crystallization from 1:1 $CHCl_3$/petroleum-ether gave **7** as a colorless solid in 67% yield (4.10 g), mp 180–182 °C. IR (KBr, ν, cm^{-1}): 3035, 1601, 1539, 1492, 1437, 1293, 1223, 1056, 1044, 884, 757, 783, 711, 679, 605, 566. ^{1}H NMR (300 MHz, $CDCl_3$): δ 8.14 (d, J=7.5 Hz, 2H, Ar–*H*), 7.97 (d, J=8.1 Hz, 2H, Ar–*H*), 7.70 (t, J=6.9 Hz, 2H, Ar–*H*), 7.62 (t, J=6.9 Hz, 2H, Ar–*H*), 5.20 (s, 4H, Ar–CH_2Br). *m/z*: 409 (M+1)$^+$, 407, 391, 375, 369, 346, 332, 329, 327, 298, 258, 252, 242, 233, 224. Anal. Calcd for $C_{16}H_{12}Br_2N_2O$: C, 47.06; H, 2.94; N, 6.86; Br, 39.21. Found: C, 47.32; H, 3.10; N, 6.66; Br, 39.42%.

4.1.6. *N*-[2,5-Bis(2-methylphenyl)-1,3,4-oxadiazole]aza-15-crown-5 (OBOX). This reaction was carried out as described for **OMOX** by using dibromide **7** (0.408 g, 1 mmol), monoaza-15-crown-5 (0.657 g, 3 mmol), and anhyd K_2CO_3 (0.552 g, 4 mmol) in 10 mL of dry MeCN. The brown oily mass obtained was extracted with chloroform, washed with water, and the organic layer dried over anhyd Na_2SO_4. Crude oily product obtained upon solvent removal was purified by SiO_2 column chromatography (R_f=0.21) using $CHCl_3$/CH_3OH (98:2) as an eluent. The compound **OBOX** was obtained as pale yellow oil in 55% yield (0.376 g). IR (Nujol, ν, cm^{-1}): 3065, 2963, 1615, 1552, 1496, 1443, 1311, 1270, 1200, 1088, 974, 851, 751, 715, 624. ^{1}H NMR (300 MHz, $CDCl_3$): δ 7.94 (d, J=8.7 Hz, 2H, Ar–*H*), 7.90 (d, J=8.4 Hz, 2H, Ar–*H*), 7.53 (t, J=6.7 Hz, 2H, Ar–*H*), 7.39 (t, J=6.9 Hz, 2H, Ar–*H*), 4.22 (s, 4H, >NCH_2–Ar), 3.51–3.71 (m, 32H, –OCH_2CH_2–), 2.82 (t, J=5.5 Hz, 8H, >NCH_2CH$_2$O–). ^{13}C NMR ($CDCl_3$): δ 164.39, 131.53 130.36, 129.61, 129.49, 127.22, 122.89, 71.12, 70.73, 70.37, 70.10, 59.09, 55.02. *m/z*: 687 (M+3)$^+$, 673, 578, 507, 467, 423, 374, 290, 265, 157. Anal. Calcd for $C_{36}H_{52}N_4O_9$: C, 63.16; H, 7.60; N, 8.18. Found: C, 62.95; H, 7.89; N, 8.42%.

Acknowledgements

Thanks are due to BRNS, Government of India for financial support in the form of research grant 2004/37/29/BRNS.

References and notes

1. Andrews, G. K. *BioMetals* **2001**, *14*, 223–237.
2. Truong-Tran, A. Q.; Carter, J.; Ruffin, R. E.; Zalewski, P. D. *BioMetals* **2001**, *14*, 315–330.
3. Lippard, S. J.; Berg, J. M. *Principles of Bioinorganic Chemistry*; University Science Books: Mill Valley, CA, 1994.
4. Cuajungco, M. P.; Lees, G. J. *Neurobiol. Dis.* **1997**, *4*, 137–169.
5. Ravanti, L.; Kahari, V. M. *Int. J. Mol. Med.* **2000**, *6*, 391–407.
6. (a) Voegelin, A.; Pfister, S.; Scheinost, A. C.; Marcus, M. A.; Kretzschmar, R. *Environ. Sci. Technol.* **2005**, *39*, 6616–6623; (b) Callender, E. *Environ. Sci. Technol.* **2000**, *34*, 232–238; (c) Nowicki, J. L.; Johnson, K. S.; Coale, K. H.; Elrod, V. A.; Lieberman, S. H. *Anal. Chem.* **1994**, *66*, 2732–2738.
7. Frederickson, C. J.; Kasarskis, E. J.; Ringo, D.; Frederickson, R. E. *J. Neurosci. Methods* **1987**, *20*, 91–103.
8. Zalewski, P. D.; Forbes, I. J.; Betts, W. H. *Biochem. J.* **1993**, *296*, 403–408.
9. Taki, M.; Wolford, J. L.; O'Halloran, T. V. *J. Am. Chem. Soc.* **2004**, *126*, 712–713.
10. (a) Chang, C. J.; Nolan, E. M.; Jaworski, J.; Okamoto, K.-I.; Hayashi, Y.; Sheng, M.; Lippard, S. J. *Inorg. Chem.* **2004**, *43*, 6774–6779; (b) Chang, C. J.; Nolan, E. M.; Jaworski, J.; Burdette, S. C.; Sheng, M.; Lippard, S. J. *Chem. Biol.* **2004**, *11*, 203–210; (c) Burdette, S. C.; Frederickson, C. J.; Bu, W.; Lippard, S. J. *J. Am. Chem. Soc.* **2003**, *125*, 1778–1787; (d) Walkup, G. K.; Spingler, B.; Tsien, R. Y.; Lippard, S. J. *J. Am. Chem. Soc.* **2001**, *123*, 7831–7841; (e) Walkup, G. K.; Burdette, S. C.; Lippard, S. J.; Tsien, R. Y. *J. Am. Chem. Soc.* **2000**, *122*, 5644–5645.
11. (a) Parola, A. J.; Lima, J. C.; Pina, F.; Pina, J.; de Melo, J. S.; Soriano, C.; García-España, E.; Aucejo, R.; Alarcõn, J. *Inorg. Chim. Acta* **2007**, *360*, 1200–1208; (b) Kulatilleke, C. P.; de Silva, S. A.; Eliav, Y. *Polyhedron* **2006**, *25*, 2593–2596; (c) Gan, W.; Jones, S. B.; Reibenspies, J. H.; Hancock, R. D. *Inorg. Chim. Acta* **2005**, *358*, 3958–3966; (d) Fan, J.; Peng, X.; Wu, Y.; Lu, E.; Hou, J.; Zhang, H.; Zhang, R.; Fu, X. *J. Lumin.* **2005**, *114*, 125–130; (e) Wang, J.; Xiao, Y.; Zhang, Z.; Qian, X.; Yanga, Y.; Xu, Q. *J. Mater. Chem.* **2005**, *15*, 2836–2839; (f) Jiang, P.; Guo, Z. *Coord. Chem. Rev.* **2004**, *248*, 205–229; (g) Lakshmi, C.; Hanshaw, R. G.; Smith, B. D. *Tetrahedron* **2004**, *60*, 11307–11315; (h) Kikuchi, K.; Komatsu, K.; Nagano, T. *Curr. Opin. Chem. Biol.* **2004**, *8*, 182–191; (i) Frederickson, C. J.; Burdette, S. C.; Frederickson, C. J.; Sensi, S. L.; Weiss, J. H.; Yin, H. Z.; Balaji, R. V.; Truong-Tran, A. Q.; Bedell, E.; Prough, D. S.; Lippard, S. J. *J. Neurosci. Methods* **2004**, *139*, 79–89.
12. (a) Parkesh, R.; Lee, T. C.; Gunnlaugsson, T. *Org. Biomol. Chem.* **2007**, *5*, 310–317; (b) Ngwendson, J. N.; Amiot, C. L.; Srivastava, D. K.; Banerjee, A. *Tetrahedron Lett.* **2006**, *47*, 2327–2330; (c) Meng, X.-M.; Zhu, M.-Z.; Liu, L.; Guo, Q.-X. *Tetrahedron Lett.* **2006**, *47*, 1559–1562; (d) Ohshima, A.; Momotake, A.; Arai, T. *Tetrahedron Lett.* **2004**, *45*, 9377–9381; (e) Gunnlaugsson, T.; Lee, T. C.; Parkesh, R. *Tetrahedron* **2004**, *60*, 11239–11249; (f) Gunnlaugsson, T.; Lee, T. C.; Parkesh, R. *Org. Lett.* **2003**, *5*, 4065–4068; (g) Kimura, E.; Koike, T. *Chem. Soc. Rev.* **1998**, *27*, 179–184.
13. (a) Xue, G.; Bradshaw, J. S.; Dalley, N. K.; Savage, P. B.; Izatt, R. M.; Prodi, L.; Montalti, M.; Zaccheroni, N. *Tetrahedron* **2002**, *58*, 4809–4815; (b) Jefferson, J. R.; Hunt, J. B.; Ginsburg, A. *Anal. Biochem.* **1990**, *187*, 328–336; (c) Grynkiewicz, G.; Poenie, M.; Tsien, R. Y. *J. Biol. Chem.* **1985**, *260*, 3440–3450.
14. (a) Liu, Y.; Zhang, N.; Chen, Y.; Wang, L.-H. *Org. Lett.* **2007**, *9*, 315–318; (b) Park, M. S.; Swamy, K. M. K.; Lee, Y. J.; Lee, H. N.; Jang, Y. J.; Moon, Y. H.; Yoon, J. *Tetrahedron Lett.* **2006**, *47*, 8129–8132; (c) Zhang, G.-Q.; Yang, G.-Q.; Zhua, L.-N.; Chen, Q.-Q.; Ma, J.-S. *Sens. Actuators B: Chem.* **2006**, *114*, 995–1000; (d) Mikata, Y.; Wakamatsu, M.; Kawamura,

A.; Yamanaka, N.; Yano, S.; Odani, A.; Morihiro, K.; Tamotsu, S. *Inorg. Chem.* **2006**, *45*, 9262–9268; (e) Wu, Y.; Peng, X.; Guo, B.; Fan, J.; Zhang, Z.; Wang, J.; Cui, A.; Gao, Y. *Org. Biomol. Chem.* **2005**, *3*, 1387–1392.

15. (a) Lim, N. C.; Freake, H. C.; Brueckner, C. *Chem.—Eur. J.* **2004**, *11*, 38–49; (b) Canzoniero, L. M. T.; Sensi, S. L.; Choi, D. W. *Neurobiol. Dis.* **1997**, *4*, 275–279; (c) Atar, D.; Backx, P. H.; Appel, M. M.; Gao, W. D.; Marban, E. *J. Biol. Chem.* **1995**, *270*, 2473–2477.
16. (a) Costero, A. M.; Gil, S.; Sanchis, J.; Peransi, S.; Sanz, V.; Williams, J. A. G. *Tetrahedron* **2004**, *60*, 6327–6334; (b) Kawakami, J.; Miyamoto, R.; Kimura, K.; Obata, K.; Nagaki, M.; Kitahara, H. *J. Comput. Chem. Jpn.* **2003**, *2*, 57–62.
17. (a) Kateinopoulos, H. E. *Curr. Pharm. Design* **2004**, *10*, 3835–3852; (b) Bratton, L. D.; Strzelbicka, B.; Bartsch, R. A. *Arkivoc* **2003**, *13*, 80–88.
18. (a) Mashraqui, S. H.; Subramanian, S.; Bhasikuttan, A. C. *Tetrahedron* **2007**, *63*, 1680–1688; (b) Mashraqui, S. H.; Subramanian, S.; Tabrez, K. *Chem. Lett.* **2006**, *35*, 786–787; (c) Mashraqui, S. H.; Kumar, S.; Vashi, D. *J. Inclusion Phenom. Macro. Chem.* **2004**, *48*, 125–130.
19. Mashraqui, S. H.; Subramanian, S.; Bhasikuttan, A. C.; Kapoor, S.; Sapre, A. V. *Sens. Actuators B: Chem.* **2007**, *122*, 347–350.
20. (a) Yang, N. C.; Jeong, J. K.; Suh, D. H. *Chem. Lett.* **2003**, *32*, 40–41; (b) Mitschke, U.; Bäuerle, P. *J. Mater. Chem.* **2000**, *10*, 1471–1507.
21. Jyotirmayee, M.; Pal, H.; Sapre, A. V. *Bull. Chem. Soc. Jpn.* **1999**, *72*, 2193–2202.
22. (a) Shin-ichi, K.; Kinjo, T.; Yano, Y. *Tetrahedron Lett.* **2005**, *46*, 3183–3186; (b) Fery-Forgues, S.; Al-Ali, F. *J. Photochem. Photobiol. C: Rev.* **2004**, *5*, 139–153 and references cited therein; (c) Geue, J. P.; Head, N. J.; Ward, D.; Lincoln, S. F. *Dalton Trans.* **2003**, 521–526; (d) Kim, S. K.; Bang, M. Y.; Lee, S.-H.; Nakamura, K.; Cho, S.-W.; Yoon, J. *J. Inclusion Phenom. Macro. Chem.* **2002**, *43*, 71–75.
23. Kubo, K.; Mori, A. *J. Mater. Chem.* **2005**, *15*, 2902–2907 and references cited therein.
24. Mohanty, J.; Bhasikuttan, A. C.; Nau, W. M.; Pal, H. *J. Phys. Chem. B* **2006**, *110*, 5132–5138.
25. Bartsch, R. A.; Yang, I. W.; Jeon, E. G.; Walkowiak, W.; Charewicz, W. A. *J. Coord. Chem.* **1992**, *27*, 75–85.